ELSEVIER

Journal of Alloys and Compounds 441 (2007) 291–296

Journal of ALLOYS AND COMPOUNDS

www.elsevier.com/locate/jallcom

Synthesis and magnetic properties of concentrated α-Fe_2O_3 nanoparticles in a silica matrix

Marin Tadić [a,*], Dragana Marković [a], Vojislav Spasojević [a], Vladan Kusigerski [a], Maja Remškar [b], Janez Pirnat [c], Zvonko Jagličić [c]

[a] *Condensed Matter Physics Laboratory, The Vinča Institute, POB 522, 11001 Belgrade, Serbia and Montenegro*
[b] *Jožef Stefan Institute, Jamova 39, 1000 Ljubljana, Slovenia*
[c] *Institute of Mathematics, Physics and Mechanics, Jadranska 19, 1000 Ljubljana, Slovenia*

Received 26 May 2006; received in revised form 20 September 2006; accepted 25 September 2006
Available online 13 November 2006

Abstract

Hematite nanoparticles in a silica matrix containing 30 wt.% of hematite were synthesized by the sol–gel method. Transmission electron microscopy studies showed that the average particle size of the hematite was about 4 nm with a narrow size distribution, while selected area electron diffraction confirmed the formation of the hematite phase. Investigation of the magnetic properties by DC magnetization and AC susceptibility measurements indicated behavior typical of a superparamagnetic system, such as the existence and frequency dependence of a blocking temperature, irreversibility of the zero-field-cooled (ZFC) and field-cooled (FC) curves, and emergence of magnetic hysteresis below the blocking temperature. Quantitative analysis of the DC magnetic data indicated that the system consisted of an assembly of superparamagnetic nanoparticles with a narrow size distribution, while the AC data implied the existence of weak inter-particle interactions.

PACS: 61.46.Df; 68.37.Lp; 75.20.-g

Keywords: Nanostructured materials; Sol–gel processes; Magnetization; Magnetic measurements; Transmission electron microscopy, TEM

1. Introduction

In the last few years nanoparticles of iron oxides have evoked remarkable interest from both theoretical aspects and their wide range of potential applications in nanodevices. Great attention was devoted to the ferrimagnetic γ-Fe_2O_3 (maghemite) [1,2] and antiferromagnetic α-Fe_2O_3 (hematite) [3–5] nanoparticle systems. In particular, maghemite has been widely used in magnetic recording systems and catalysis [6,7], whereas hematite has been used in pigments, catalytic reactions and as an anticorrosive agent [8].

Hematite crystallizes in the trigonal system, space group *R*-3*c* [9]. Its magnetic properties have been studied extensively both in bulk and nanoparticle form. In bulk hematite below the Néel temperature T_N ($948 < T_N < 963$ K) [10], the Morin transition takes place as a first order magnetic transition at the temperature $T_M \sim 263$ K [10,11]. Below T_M spins are oriented in antiparallel directions along the trigonal (1 1 1) axis (*c*-axis), and the material behaves as a uniaxial antiferromagnet [12]. Above T_M, spins show slight canting with respect to the basal (1 1 1) plane and a small net magnetic moment appears (weak ferromagnetism) [13,14]. As the size of the hematite particle decreases and enters the nanometre scale, the magnetic properties change and new phenomena appear. Consequently, nanoparticle hematite is an even more interesting material for fundamental research because it can display three critical temperatures: the Néel temperature, the Morin temperature and the blocking temperature [15]. The Morin temperature decreases as the particle size decreases, tending to disappear for particles smaller than about 8–20 nm [16,17]. Crystal defects, strains, stoichiometric deviations and surface effects also tend to reduce the Morin temperature [11,18]. If the particles become small enough, the magnetic moment in a single domain fluctuates in direction due to thermal agitation, leading to superparamagnetic behavior above the blocking temperature T_B, and to spatial freezing of these moments below T_B.

* Corresponding author. Tel.: +381 11 8065828; fax: +381 11 8065829.
E-mail address: marint@vin.bg.ac.yu (M. Tadić).

0925-8388/$ – see front matter © 2006 Elsevier B.V. All rights reserved.
doi:10.1016/j.jallcom.2006.09.099

Nanostructured hematite in various forms, such as nanoparticles embedded in an inert matrix, nanowires, nanorods and nanotubes has been widely studied in order to understand the influence of size, shape, anisotropy, dipole–dipole interactions, exchange interactions and surface effects on its magnetic properties [3–5,19–23]. To allow contributions from the above effects to be distinguished, the principal aim in the syntheses of nanoparticles is to obtain particles with well-defined morphology and size, and also with a narrow size distribution. In addition, the possibility of controlling the presence of inter-particle interactions is also desirable. Since nanocomposites consisting of hematite nanoparticles embedded in an insulating matrix (silica, alumina and polymers) fulfil most of the above requirements, interest in these materials has grown considerably in recent years [3,4,19,24]. Special attention has been paid to the impact of inter-particle interactions on the magnetic properties of these systems, with a wide variety of experimental techniques employed in these investigations, such as Mössbauer spectroscopy, AC susceptibility, DC magnetization and neutron scattering [3,4,19,20,25].

Among other preparative techniques the sol–gel process has proved to be a convenient method for the synthesis of nanocomposites. Various nanoparticles dispersed in a silica matrix have been successfully synthesized by the sol–gel method, such as Fe [26], Ni [27], γ-Fe_2O_3 [28], NiZn-ferrite [29] and α-Fe_2O_3 [30]. Silica provides a convenient matrix for fundamental investigations because its cavities have a well-defined size and geometry, and they are also regularly arranged in space. Considerable attention has been paid to the influence of the processing parameters such as the concentration of components, pH of the solution, as well as the heat treatment temperature and duration on the physical and chemical properties of these materials.

The aim of this work was to obtain a relatively high concentration of hematite nanoparticles in an amorphous silica matrix by the sol–gel method, and to investigate the magnetic properties of the system obtained. The required features were a small particle size of a few nanometres with a narrow size distribution and uniform dispersion. The target composition was chosen to have a weight ratio α-$Fe_2O_3/(\alpha$-$Fe_2O_3 + SiO_2)$ of 30%. This ratio lies in between the highly concentrated nanocomposite α-Fe_2O_3/Al_2O_3 (68% in weight) possessing strong magnetic inter-particle interactions [4], and the diluted α-Fe_2O_3/polymer nanocomposite (14% in weight) with negligible magnetic interactions [3].

2. Experimental

The α-Fe_2O_3/SiO_2 nanocomposite containing 30 wt.% of α-Fe_2O_3 was prepared using the conventional sol–gel method. An ethanol solution of tetraethoxysilane (TEOS, Aldrich 98%) was mixed with an aqueous solution of iron nitrate ($Fe(NO_3)_3{\cdot}9H_2O$, Aldrich 98%), with HNO_3 as an acid catalyst. The mole ratios of ethanol to TEOS and water to TEOS were 4:1 and 11.67:1, respectively. After 1 h of stirring the pH of the mixture was about 2. The clear sol was poured into a glass beaker and allowed to gel in the air. The gel was dried for about one week with temperature slowly increasing up to 80 °C, and afterwards the sample was heated in air at 400 °C for 5 h.

The microstructure of this material was investigated by high resolution transmission electron microscopy, using a JEOL 2010 F instrument.

Magnetic measurements were performed on a commercial SQUID-based magnetometer (Quantum Design MPMS XL-5) over a wide range of temperatures (2–300 K) and applied DC fields (up to 5 T). The same instrument was used for AC magnetization measurements carried out in the $1\ \text{Hz} \leq \nu \leq 1000\ \text{Hz}$ frequency range in a temperature region encompassing the blocking temperatures. The diamagnetic contribution of the silica matrix was subtracted from the recorded magnetic data.

3. Results and discussion

A transmission electron micrograph (TEM) and the corresponding selected area electron diffraction (SAED) pattern are shown in Fig. 1. The TEM micrograph indicates formation of nanoparticles of an average size of about 4 nm, and it also shows their uniform dispersion in the amorphous silica matrix, Figs. 1(a) and (b). The selected area electron diffraction pattern shown in Fig. 1(c) consists of diffraction spots/rings that were indexed in correspondence to the rhombohedral hematite structure (72-469 JCPDS-ICDD).

The zero-field-cooled (ZFC) and the field-cooled (FC) magnetization curves measured in the low DC field of 50 Oe are shown in Fig. 2. The sample did not exhibit the Morin transition down to 2 K, as expected for small particles less than 5 nm diameter in according to the literature data [3]. From Fig. 2, it can be concluded that behavior typical of magnetic nanoparticles was obtained. The ZFC curve exhibits a relatively narrow maximum with the peak value at the temperature $T_B = 19$ K. Below T_B the ZFC magnetization decreases sharply, while the FC magnetization increases continuously below T_B down to 2 K, which is usually considered to be characteristic of non-interacting nanoparticles [3,27]. On the other hand, the plateau in the FC magnetization curve below T_B observed in nanosized α-Fe_2O_3 points to the existence of strong inter-particle interactions [4,5] that can also produce the increase of T_B [4,31]. Our T_B value is comparable to the value of $T_B \approx 22$ K reported for diluted hematite nanoparticles with 5 nm mean size [3]. The ZFC and FC curves do not coincide even in a field of 5 T (Fig. 2, inset) thus indicating the presence of a large amount of anisotropy energy.

The irreversibility temperature T_{irr} at which the ZFC and FC curves begin to separate corresponds to the blocking temperature of the largest particles in the system. T_{irr} is usually determined as the point where the ratio $(M_{FC} - M_{ZFC})/M_{FC}$ is less than 1% [32], and this criterion gives a value of $T_{irr} = 45$ K for our sample. The difference between T_{irr} and T_B is considered to be a qualitative measure of the width of the nanoparticles size distribution [3]. In our case this difference is not large, thus indicating a narrow size distribution.

The field dependence of isothermal magnetization was recorded at 10 K, i.e. below T_B, in the field range of ± 5 T. From Fig. 3, it can be seen that for high field values magnetization increases almost linearly, showing a lack of magnetic saturation. The hysteresis loop obtained is symmetric around the origin (Fig. 3, inset), with the values of coercive field and remanence magnetization $H_C = 610$ Öe and $M_r = 0.435$ emu/g, respectively. These values are comparable with those for α-Fe_2O_3 nanoparticle systems reported in the literature [3,5]. Hysteretic behaviour is a consequence of surface spin disorder, while the linear part

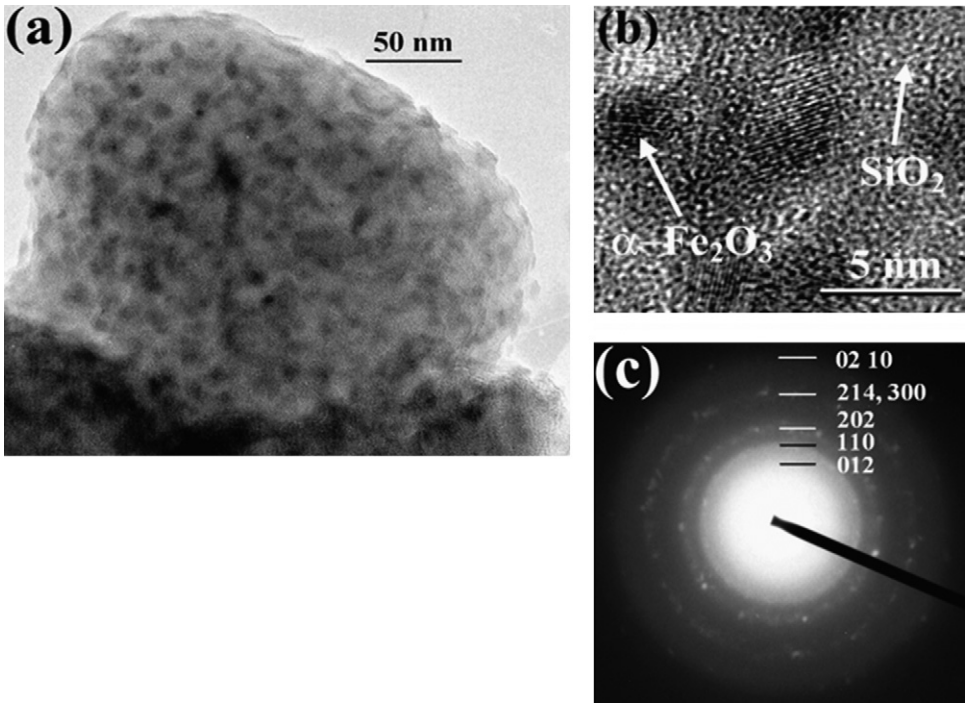

Fig. 1. Transmission electron micrograph of α-Fe_2O_3/SiO_2: (a) silica grain with embedded α-Fe_2O_3 nanoparticles; (b) high-resolution image of the selected grain region; (c) the SAED pattern of the same region.

of the $M(H)$ dependence represents the contribution of the particle's antiferromagnetic core.

To check the superparamagnetic behavior of our sample, we performed $M(H)$ measurements in the field range 0–5 T at several temperatures above $T_{irr} = 45$ K. From the data presented in Fig. 4(a), it can be seen that magnetic hysteresis disappears at the temperature of 50 K. The same magnetization data are presented in Fig. 4(b) as a function of H/T. If the sample were truly superparamagnetic, then the magnetization curves measured at different temperatures could be superimposed when magnetization is plotted as a function of H/T [33]. This feature is indeed achieved as can be seen in Fig. 4(b), thus confirming the superparamagnetic behavior of our sample for temperatures above 50 K.

Superparamagnetism can be described by the Langevin theory of paramagnetism where magnetization dependence on both temperature and field is given by [33]:

$$M(H, T) = M_S L \left[\frac{m_p H}{k_B T}\right] \quad (1)$$

In this expression, M_S is the saturation magnetization, L the Langevin function and m_p is the particle's magnetic moment. The above expression assumes that the system consists of non-interacting and monodisperse particles. By fitting $M(H)$ data to expression (1), where M_S and m_p are considered as fitting

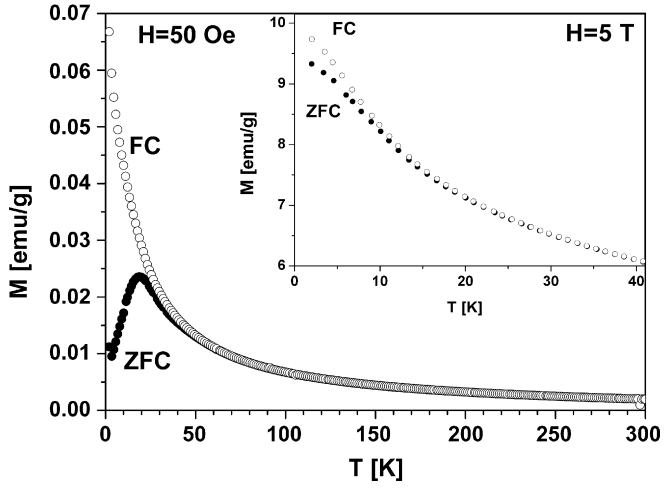

Fig. 2. Temperature dependence of the zero-field-cooled (ZFC, solid symbols) and field-cooled (FC, open symbols) magnetization measured in a field of 50 Oe and 5 T (inset).

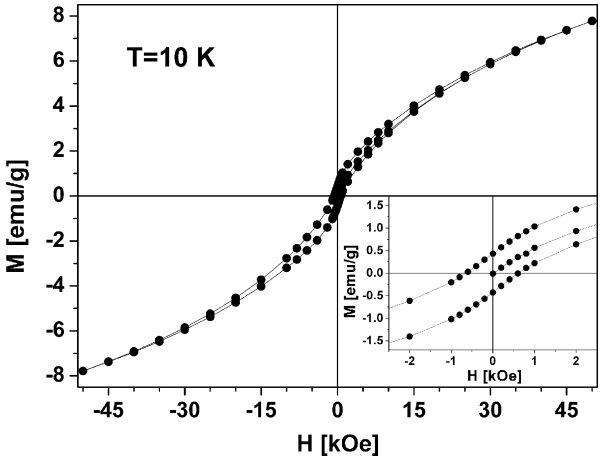

Fig. 3. Magnetization vs. field dependence recorded at 10 K. The inset shows low field magnetization behavior.

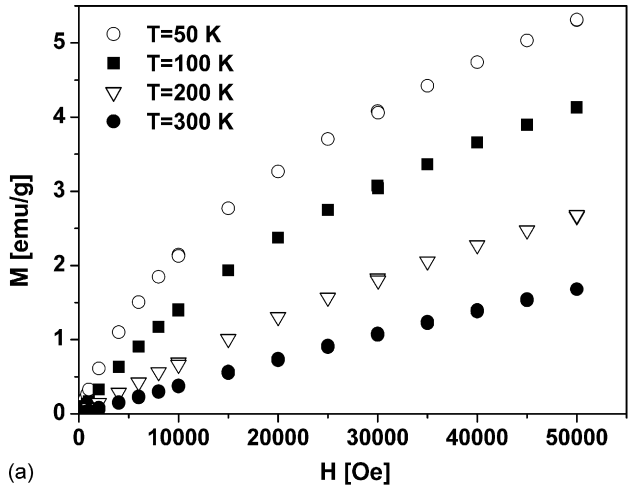

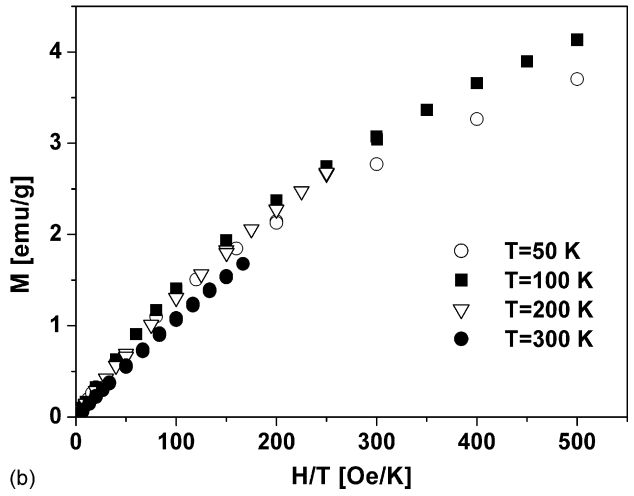

Fig. 4. Magnetization of α-Fe_2O_3 nanoparticles at several temperatures expressed as a function of the applied field H (a) and as a function of H/T (b).

parameters, information on the magnetic moment of the superparamagnetic particles can be obtained. Estimation of the mean particle size can be made by using the following expression for the magnetic moment of a particle:

$$m_p = \frac{\pi d^3 M_S}{6}, \tag{2}$$

which assumes the particle has a spherical shape, and where d denotes the diameter of the sphere.

The fit of Eq. (1) to $M(H)$ data measured at 300 K is shown in Fig. 5, where the fitting parameters obtained are $M_S = 4$ emu/g and $m_p = 121\ \mu_B$. The prevailing contribution to the value of m_p can be attributed to disorder of the surface magnetic structure. Also, for very small hematite particles of a few nano-meter in size, the existence of non-exact compensation of the magnetic moments in the antiferromagnetic core is also expected to contribute to m_p [4]. From the values for M_S and m_p obtained and Eq. (2), the mean particle diameter was determined to be $d = 4.6$ nm. This value determined by applying Langevin's theory is consistent with the mean particle diameter obtained from TEM micrographs.

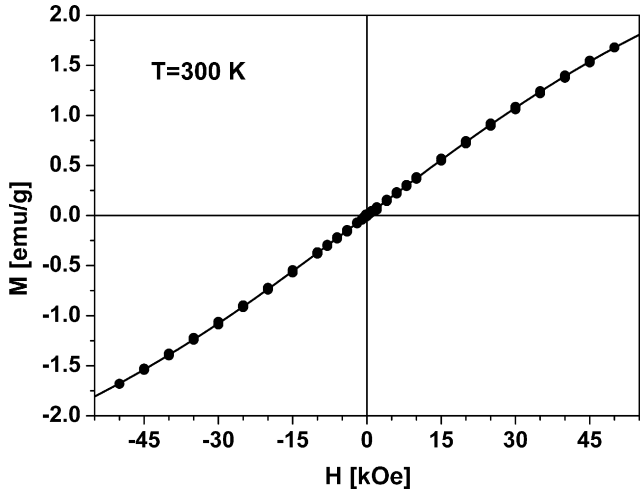

Fig. 5. Langevin function fit (full line) to the $M(H)$ data (dots) measured at 300 K.

In order to investigate the presence of inter-particle interactions, we performed AC susceptibility measurements at four different frequencies in the 1–1000 Hz range, and in the temperature range 5–40 K that encompasses the blocking temperature of our sample. From the data presented in Fig. 6, it can be seen that the in-phase part $\chi'(T)$ is frequency dependent in a way that the peak position (corresponding to the blocking temperature T_B) increases with increasing frequency, while the height of the peak decreases with increasing frequency.

According to the Néel theory of superparamagnetism [34], the magnetic moments of non-interacting single domain identical particles with uniaxial anisotropy fluctuate between two directions of easy axes with a relaxation time τ that obeys the Arrhenius law:

$$\tau = \tau_0 \exp\left(\frac{\Delta E}{k_B T}\right), \tag{3}$$

where ΔE is the energy barrier to moment reversal in a single particle and τ_0 is the so-called attempt frequency. In the case

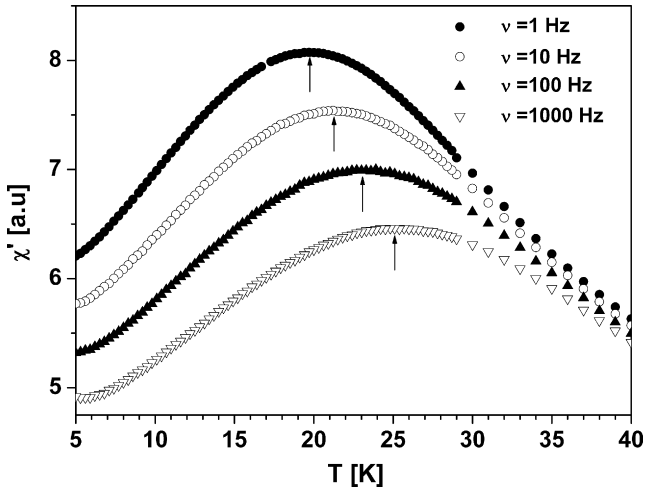

Fig. 6. Temperature dependence of the real part of the AC susceptibility at different frequencies. Arrows denote positions of T_B.

Table 1
Comparative review of magnetic parameters of several distinct nanosized α–Fe_2O_3 systems

Sample	Mean particle size (nm)	T_B (K)	T_M (K)	m_p [μ_B]	K (erg/cm^3)	Inter-particle interactions	Ref.
α-Fe_2O_3 in polymer matrix	$d \sim 5$	~22	none	~80	8×10^5	No	[3]
α-Fe_2O_3 nanowires	$d \sim$ 10–20, 1 ~ 10–20 μm	~120	<4	–	–	Yes	[5]
α-Fe_2O_3 in alumina matrix	$d \sim 3$	~145	<5	~40	–	Yes	[4]
α-Fe_2O_3							
As-prepared	$d \sim 40$	~390	177	~13200	1.1×10^5	Yes	[14]
Annealed		~845	205	~11500	2.6×10^5		
α-Fe_2O_3 in silica matrix	$d \sim 4$	~19	none	~120	1.6×10^6	Yes	This work

of AC measurements τ corresponds to the measurement time and thus it is the inverse of the measurement frequency ν. From Eq. (3), it follows that in the case of non-interacting particles the dependence of $\ln \nu$ versus ${T_B}^{-1}$ should be linear, while the attempt frequency τ_0 is usually within the range from 10^{-9} to 10^{-12} [35]. The value of $\tau_0 \sim 10^{-15}$ s determined from the fit of our experimental data to the Arrhenius law (Fig. 7) is much lower than the above quoted limit. This indicates the existence of inter-particle interactions in our system.

Further evidence for the presence of interactions can be gained from the empirical parameter $C_1 = \Delta T_B/(T_B\ \Delta \log \nu)$, where T_B denotes the average value of blocking temperatures in the range of experimental frequencies, while ΔT_B denotes the difference between the maximum and minimum value of T_B (Fig. 6). In this way a value of C_1 equal to 0.08 was obtained.

In the case of interacting particles, the frequency dependence of T_B should obey the Vogel-Fulcher law [35]:

$$\tau = \tau_0 \exp\left[\frac{E_a}{k_B(T - T_0)}\right], \quad (4)$$

where $\tau = 1/\nu$, E_a is the activation energy and parameter T_0 is a measure of the inter-particle interaction strength. The fit of the experimental data to Eq. (4) is given in the inset of Fig. 7, where the following values of fitting parameters were obtained: $\tau_0 = 2.5 \times 10^{-12}$ s, $E_a/k_B = 400$ K, $T_0 = 4$ K. All the parameters obtained have reasonable physical values [3,36]. The

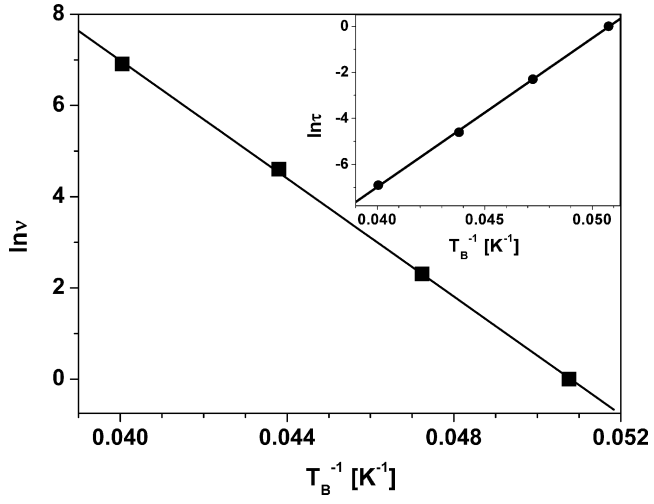

Fig. 7. Change of blocking temperatures T_B with AC field frequency ν fitted to the Arrhenius function. Inset: fit to the Vogel-Fulcher function.

magnetic anisotropy parameter E_a/k_B can be used to estimate the anisotropy constant K, using the relation $KV = E_a$, where V denotes the volume of a particle. For a spherical particle with diameter $d = 4$ nm, this relation gives $K = 1.6 \times 10^6$ erg/cm^3, while the value for bulk hematite is $K = 8 \times 10^4$ erg/cm^3 [37]. This enhancement observed for nanoparticles is customarily attributed to surface effects [3].

Using the T_0 value obtained from the Vogel-Fulcher fit, we can calculate the value of another empirical parameter $C_2 = (T_B - T_0)/T_B = 0.82$. In the case of non-interacting superparamagnetic particles the parameters C_1 and C_2 have approximate values of 0.1 and 1, respectively [32]. Also, both C_1 and C_2 decrease with increasing interactions [38]. Since the parameters C_1 and C_2 obtained for our hematite nanocomposite have lower values than is usual for a non-interacting superparamagnetic system, the presence of inter-particle interactions can be inferred. Because of the small magnetic moment of the antiferromagnetic nanoparticles, dipole–dipole interactions are generally weak and consequently the exchange interactions between surface atoms of neighbouring particles are expected to make the prevailing contribution to the interparticle interaction [39].

Table 1 provides a comparative review of values of T_B, T_M, m_p and K for different nanoparticle α-Fe_2O_3 systems. It can be noticed that values of T_B are mostly influenced by the particle size as well as inter-particle interactions. The dependence of T_M, m_p and K on the particle size is also noticeable. The values obtained for the system considered in this work show the closest similarities to the corresponding parameters for the non-interacting nanohematite system reviewed in reference [3]. On the basis of the above comparisons, we can claim that inter-particle interactions in our system are of weak intensity.

4. Conclusion

An α-Fe_2O_3/SiO_2 nanocomposite containing 30 wt.% of α-Fe_2O_3 was prepared by the sol–gel method and characterized by using transmission electron micrography and SQUID magnetometry. The hematite nanoparticles obtained, with an average particle size of about 4 nm, were evenly dispersed in an amorphous silica matrix and TEM micrography did not show evidence of significant particle agglomeration. Selected area electron diffraction confirmed formation of the hematite phase. Both DC magnetization and AC susceptibility experiments showed behavior characteristic of an assembly of superparamagnetic

particles. The particle moments thermally fluctuated freely in the high-temperature superparamagnetic state (above 50 K), and they were blocked below the average blocking temperature of $T_B \approx 19$ K. The temperature and field dependence of magnetization in the superparamagnetic regime satisfactorily fitted Langevin's theory of paramagnetism. The mean particle size determined from this fit was very close to particle size determined by TEM. The AC susceptibility measurements revealed the existence of weak inter-particle interactions resulting from the high concentration of nanosize magnetic grains in the silica matrix.

Acknowledgement

The Serbian Ministry of Science, Technology and Development supported this work financially.

References

[1] P. Dutta, A. Manivannan, M.S. Seehra, Phys. Rev. B 70 (2004) 174428-1.
[2] C. Caizer, I. Hrianca, Eur. Phys. J. B 31 (2003) 391.
[3] R.D. Zysler, M. Vasquez Mansilla, D. Fiorani, Eur. Phys. J. B 41 (2004) 171.
[4] R.D. Zysler, D. Fiorani, A.M. Testa, J. Magn. Magn. Mater. 224 (2001) 5.
[5] Y.Y. Xu, X.F. Rui, Y.Y. Fu, H. Zhang, Chem. Phys. Lett. 410 (2005) 36.
[6] A.M. Testa, S. Foglia, L. Suber, D. Fiorani, L. Casas, R. Roig, E. Molins, J.M. Grenèche, J. Tejada, J. Appl. Phys. 90 (2001) 1534.
[7] F. Hong, B.L. Yang, L.H. Schwartz, H.H. Kung, J. Phys. Chem. 88 (1984) 2525.
[8] F. Bondioli, A.M. Ferrari, C. Leonelli, T. Manfredini, Mater. Res. Bull. 32 (1998) 723.
[9] R.L. Blake, R.E. Hessevick, T. Zoltai, L.W. Finger, Am. Miner. 51 (1966) 123.
[10] A. Oleś, F. Kajzar, M. Kucab, W. Sikora, Magnetic Structures Determined by Neutron Diffraction, Państwowe Wydawnictwo Naukowe, Warszawa-Kraków, 1976, p. 372.
[11] F.J. Morin, Phys. Rev. 78 (1950) 819.
[12] C. Guilland, J. Phys. Radium 12 (1951) 489.
[13] J.O. Artman, J.C. Murphy, S. Foner, Phys. Rev. 138 (1965) A912.
[14] C.G. Shull, W.A. Strauser, E.O. Wollan, Phys. Rev. 83 (1951) 333.
[15] R.D. Zysler, M. Vasquez, C. Arciprete, M. Dimitrijewits, D. Rodriguez-Sierra, C. Saragovi, J. Magn. Magn. Mater. 224 (2001) 39.
[16] N. Amin, S. Arajs, Phys. Rev. B 35 (1987) 4810.
[17] R. Nininger Jr., D. Scrhroeer, J. Phys. Chem. Solids 39 (1978) 187.
[18] M.Z. Dang, D.G. Rancourt, J.E. Dutrizac, G. Lamarche, R. Provencher, Hyperfine Interact. 117 (1998) 271.
[19] D.S. Xue, C.X. Gao, Q.F. Liu, L.Y. Zhang, J. Phys.: Condens. Matter. 15 (2003) 1455.
[20] M. Vasquez-Mansilla, R.D. Zysler, C. Arciprete, M.I. Dimitrijewits, C. Saragovi, J.M. Greneche, J. Magn. Magn. Mater. 204 (1999) 29.
[21] Y. Fu, R. Wang, J. Xu, J. Chen, Y. Yan, A. Narlikar, H. Zhang, Chem. Phys. Lett. 379 (2003) 373.
[22] S. Lian, E. Wang, Z. Kang, Y. Bai, L. Gao, M. Jiang, C. Hu, L. Xu, Solid State Commun. 129 (2004) 485.
[23] X.G. Wen, S.H. Wang, Y. Ding, Z.L. Wang, S.H. Yang, J. Phys. Chem. B 109 (2005) 215.
[24] S.A. Palomares Sánchez, S. Ponce-Castañeda, J.R. Martínez, Facundo Ruiz, Yurii Chumakov, O. Domínguez, J. Non-Crystall. Solids 325 (2003) 251.
[25] F. Bødker, M.F. Hansen, C.B. Koch, K. Lefmann, S. Mørup, Phys. Rev. B 61 (2000) 10.
[26] W. Jian-Ping, L. He-Lie, J. Magn. Magn. Mater. 131 (1994) 54.
[27] F.C. Fonseca, G.F. Goya, R.F. Jardim, R. Muccillo, N.L.V. Carreño, E. Longo, E.R. Leite, Phys. Rev. B 66 (2002) 104406.
[28] C. Savii, M. Popovici, C. Enache, J. Subrt, D. Niznanski, S. Bakardzieva, C. Caizer, I. Hrianca, Solid State Ionics 151 (2002) 219.
[29] S. Ponce Castañeda, J.R. Martínez, S.A. Palomares Sánchez, F. Ruiz, J.A. Matutes Aquino, J. Sol–Gel Sci. Technol. 25 (2002) 37.
[30] I.K. Battisha, H.H. Afify, I.M. Hamada, J. Magn. Magn. Mater. 292 (2005) 440.
[31] J.L. Dormann, L. Bessois, D.J. Fiorani, J. Phys. C 21 (1988) 2015.
[32] J.A. Mydosh, Spin Glasses: An Experimental Introduction, Taylor and Francis, London, 1993, 45–118.
[33] C.M. Sorensen, in: Kenneth J. Klabunde (Ed.), Nanoscale Materials in Chemistry, Wiley-Interscience, New York, 2001, p. 205.
[34] L. Nèel, Ann. Geophys. 5 (1949) 99.
[35] S. Shtrikman, E.P. Wolfart, Phys. Lett. A 85 (1981) 467.
[36] M.I. Shliomis, V.I. Stepanov, Adv. Chem. Phys. 87 (1994) 1.
[37] A.H. Morrish, Canted Antiferromagnetism: Hematite, World Scientific, Singapure, 1994.
[38] J.L. Dorman, D. Fiorani, E. Tronc, Adv. Chem. Phys. 98 (1997) 283.
[39] M.F. Hansen, C. Bender Koch, S. Mørup, Phys. Rev. B 62 (2000) 1124.